International Journal of Scientific Research & Engineering Trends
Volume 11, Issue 1, Jan-Feb-2025, ISSN (Online): 2395-566X

# Slope Stability Analysis of Landslide at Fudale, Gamo Zone, Ethiopia

**Amanuel Abera, Bisrat Gissila, Democracy Dila, Vasudeva Rao**
Faculity of Civil Engineering, Arba Minch University Arba Minch, Ethiopia

**Abstract- Landslides are significant natural disasters that pose threats to human life and the environment, particularly in hilly regions. This study contributes to the understanding of landslide dynamics by providing localized geotechnical data and stability analyses. After the landslide in 2023, this study looks into the geotechnical conditions and stability factors that led to landslides in the Fudale, Gamo Zone, Southern Ethiopia. The research paper aims to analyze the soil characteristics contributing to landslide occurrences and to assess slope stability using the Finite Element Method (FEM) through Plaxis 2D software. Ten soil samples were collected from various depths, and laboratory tests were conducted to determine their index and engineering properties. Test results indicate that the predominant soil types are fine-grained, comprising significant percentages of clay and silt, which are particularly susceptible to saturation and subsequent landslides. The analysis identified rainfall, slope geometry, soil permeability, and groundwater conditions as critical factors influencing slope stability. The computed factor of safety (FOS) for natural conditions was found to be 0.972, indicating an unstable slope.**

**Index Terms- Landslides, Factor of Safety, FEM, Plaxis 2D, Slope Stability**

## I. INTRODUCTION

### Background

A landslide is an occurrence of a natural disaster where materials such as debris, rock, or earth mass slide down a slope, resulting in harm to both living organisms and the surrounding natural ecosystem [1]. Landslides, caused by high precipitation and weathering, are a global issue causing thousands of deaths annually, especially in tropical regions, exacerbated by demographic pressure, deforestation, and climate change [2, 3]. Ethiopia's highland regions face landslides due to diverse topography, geology, hydrology, and land-use characteristics, causing geotechnical, environmental, and socioeconomic concerns. Despite limited mitigation, infrastructure, urbanization, and land management practices increase occurrence [4].

This study investigates the slope stability of landslides in Fudale, Gamo Zone, Southern Ethiopia. The research aims to identify the geotechnical conditions contributing to landslide occurrences, determine the underlying causal factors, and assess slope stability. GIS software has been used to analyze three causal factors. The slope stability was evaluated by using Plaxis 2D software.

A landslide refers to the displacement of a large quantity of rock, debris, or soil as it drops down a slope [5]. They are a serious issue that causes thousands of deaths annually in many regions of the world [3]. High precipitation and weathering rates, especially in locations with steep topography and tectonic activity, have a severe negative impact on landslides in many regions, especially in the tropics [2]. Furthermore, as a result of increasing demographic pressure, deforestation, and land use changes [6], as well as climate change, landslide risk in the tropics is likely to rise in the near future [7]. Additionally, the majority of deaths caused by landslides happen in countries in the Global South, which are primarily found in tropical regions [8]. Furthermore, due to their significant economic, social, political, and cultural sensitivity, the impact of landslides on the people in tropical developing nations might be very substantial [9]. Because of preparatory, conditional, and triggering causative variables, mountainous locations are sensitive to mass movements. External factors that initiate mass movements, such as precipitation, seismic activity, and land utilization, are referred to as triggering causative factors.

### Factors That Are Responsible for Landslide Causes

Landslides, especially in mountainous areas, are primarily caused by water, which increases slope weight due to snowmelt or rainfall. Flooding, which is closely linked to precipitation, surface runoff, and soil saturation, is a significant factor in landslide initiation, as most moisture is derived from flood events [10]. Earthquakes cause landslides when the earth shakes and soil liquefies, causing damage to slope surfaces. As earthquake intensity increases, energy exerted on slope materials increases, leading to increased driving forces along unstable planes, causing landslides [11]. Volcanic landslides are the most destructive earth mass

failures, causing destruction to everything in their path due to the rapid descent of rock, soil, ash, and water [2, 12]. Human activities on Earth, such as infrastructure development, mining, quarrying, irrigation projects, and vegetation removal, alter Earth's mass geometry, leading to disruptions in drainage patterns and undercutting of slopes. These changes, particularly during road construction, decrease resistance to shear failure and potential mass movement [13, 2].

## II. MATERIALS AND METHODS

The research employs a combination of laboratory tests and numerical methods. Ten soil samples were collected from five test pits (TP) at depths of 1.5 to 3 meters. Key geotechnical properties, like moisture content, specific gravity, Atterberg limits, and shear strength, were analyzed by ASTM standards. Slope stability was evaluated by using the Finite Element Method (FEM) through Plaxis 2D software.

The Fudale area, situated in the Gamo zone, Southern Ethiopia Regional State, is affected by landslides in 2023. Fudale is 564 km from Addis Ababa and 54 km from Arba Minch and is surrounded by the Darashe Zone, Kamba Woreda, Arbaminch Zuria Woreda, and Bonke Woreda.

The research used various tools and software, including ArcGIS, Plaxis-2D, MS Word, and Excel, as well as devices like GPS and mobile cameras. GPS tools were used to identify landslide positions and gather pit data for slope profile analysis related to stability. ArcGIS facilitated the delineation of the research area and analysis of spatial data.

For analyzing slope stability in relation to landslides, Plaxis-2D was applied. Microsoft Word and Excel served for the analysis of laboratory data and displaying study findings.

Additionally, various laboratory test tools were used for Atterberg limits, water content, unit weight, specific gravity, grain size tests, falling head permeability tests, and triaxial tests.

**Consequence of Fudale Landslide**

**Disturbance of Environmental Features**

A landslide in Fudale caused environmental destruction, causing trees to fall, soil to fracture, and land mass to collapse. The stream, once flowing, diverted and spread across the distorted area, with some remaining at the side. The surface damage due to the landslide in the research area is shown in figure 1.

Figure 1: Surface damage due to landslide of Fudale landslide

**Socio-Economic Problems**

Land subsidence caused the destruction of banana plants and fruits in a study area, causing a landslide and pond overflow, causing damage to homes and disruption to people's livelihoods. The destruction of plants and fruits due to the landslide in the research area is shown in figure 2.

Figure 2: Destruction of plants and fruits due to landslide of Fudale Landslide

**Loss of Human Life's**

The destructive phenomenon has resulted in numerous human deaths, including pregnant women, children, elders, and cattle, as per local reports

## III. RESULTS AND DISCUSSION

Laboratory tests conducted on soil samples from five test pits indicated that the predominant soil types are fine-grained, mainly consisting of clay and silt. The specific gravity of these soils ranged from 2.67 to 2.79, confirming their classification as clayey and silty clay. The Atterberg limits showed a liquid limit (LL) between 58.75% and 67.39% and a plasticity index (PI) from 28.70% to 33.80%, indicating high plasticity and sensitivity to moisture changes, which can lead to reduced shear strength and increased susceptibility to landslides. The laboratory test results of natural moisture content (NMC) and specific gravity (GS) are shown in Table 1.

Table 1 Laboratory test results

| TP (No) | Depth (m) | NMC (%) | (GS) | Atterberg Limit | | |
|---|---|---|---|---|---|---|
| | | | | LL (%) | PL (%) | PI (%) |
| 1 | 1.5 | 37.07 | 2.71 | 64.1 | 32.55 | 31.6 |
| | 3 | 40.41 | 2.69 | 62.59 | 30.59 | 32 |
| 2 | 1.5 | 35.87 | 2.72 | 67.39 | 34.74 | 32.7 |
| | 3 | 39.14 | 2.68 | 66.71 | 32.96 | 33.8 |
| 3 | 1.5 | 38.32 | 2.69 | 59.77 | 30.57 | 29.2 |
| | 3 | 41.14 | 2.67 | 58.75 | 30.09 | 28.7 |
| 4 | 1.5 | 36.12 | 2.74 | 61.1 | 30.68 | 30.4 |
| | 3 | 39.39 | 2.7 | 60.61 | 29.39 | 31.2 |
| 5 | 1.5 | 38.21 | 2.79 | 63.4 | 32.81 | 30.6 |
| | 3 | 40.53 | 2.73 | 62.41 | 32.45 | 30 |

Table 2 Laboratory Test Results

| TP (No) | Depth (m) | Grain Size Distribution | | | | |
|---|---|---|---|---|---|---|
| | | % Gravel | % Sand | % Silt | % Clay | % Finer than 0.075 mm |
| 1 | 1.5 | 0.80 | 5.08 | 44.72 | 49.40 | 94.12 |
| | 3 | 0.26 | 6.50 | 44.09 | 49.15 | 93.24 |
| 2 | 1.5 | 0.16 | 6.98 | 50.10 | 42.76 | 92.86 |
| | 3 | 0.24 | 7.38 | 49.47 | 42.91 | 92.38 |
| 3 | 1.5 | 0.10 | 5.18 | 38.76 | 55.96 | 94.72 |
| | 3 | 0.14 | 7.38 | 37.60 | 54.88 | 92.48 |
| 4 | 1.5 | 0.24 | 7.16 | 41.39 | 51.21 | 92.6 |
| | 3 | 0.44 | 4.50 | 43.55 | 51.51 | 95.06 |
| 5 | 1.5 | 0.32 | 6.96 | 50.64 | 42.08 | 92.72 |
| | 3 | 0.34 | 6.08 | 53.53 | 40.05 | 93.58 |

Table 3 Laboratory Test Results

| TP (No) | Depth (m) | Unit Weights | | |
|---|---|---|---|---|
| | | Unit Weight (kN/m³) | Dry Unit weight (kN/m³) | Saturated Unit Weight (kN/m³) |
| 1 | 3 | 16.53 | 13.08 | 18.61 |
| 2 | 3 | 16.9 | 13.37 | 18.72 |
| 3 | 3 | 17.69 | 13.99 | 18.32 |
| 4 | 3 | 16.78 | 13.28 | 18.74 |
| 5 | 3 | 18.03 | 13.84 | 18.64 |

Table 4 Laboratory Test Results

| TP (No) | Depth (m) | Free Swell (%) | Coefficient of Permeability K(cm/sec) | Triaxial UU test | |
|---|---|---|---|---|---|
| | | | | C (kN/m2) | Ø (Degrees) |
| 1 | 3 | 26 | 4.7*10-6 | 28.02 | 9 |
| 2 | 3 | 22 | 3.63*10-6 | 50.6 | 12 |
| 3 | 3 | 30 | 2.2*10-6 | 57.6 | 16.94 |
| 4 | 3 | 40 | 1.9*10-6 | 32.12 | 15.39 |
| 5 | 3 | 30 | 2.3*10-6 | 42.54 | 13.09 |

**Determination of Elastic Modulus through Triaxial Tests**

The elastic modulus, calculated from a stress-strain curve derived from a triaxial test, was used to evaluate slope stability in soil samples, ranging from 3,394 to 5,375 kN/m². The stress-strain curves as shown in figure 1 (i & iii) and the elastic modulus can be derived from the stress-strain curves as shown in figure 1 (ii & iv).

i)

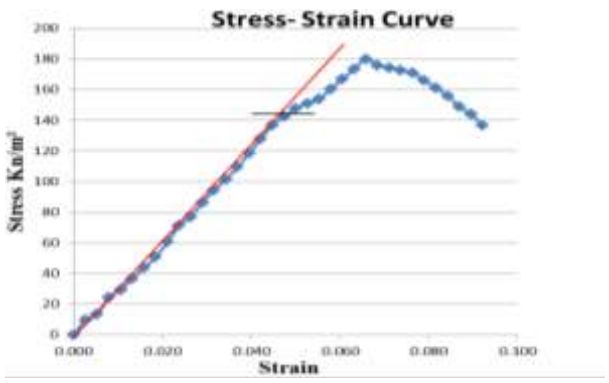


ii)

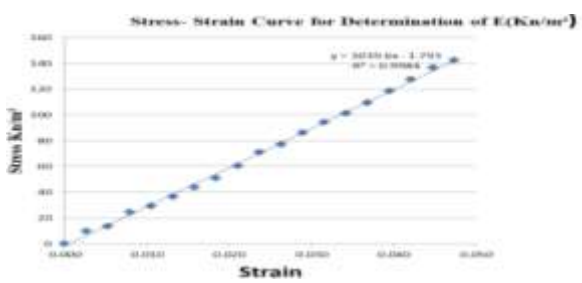

iii)

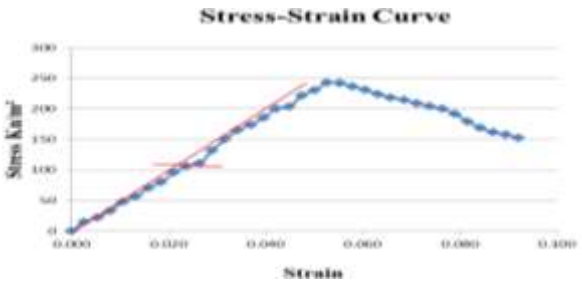


iv)

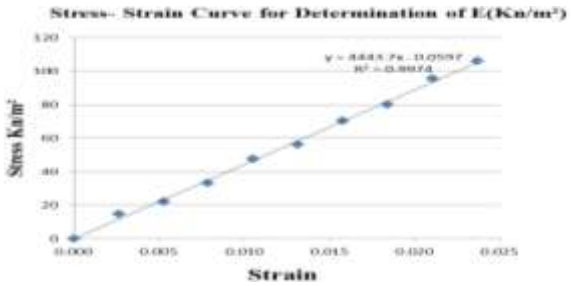


Figure 3: The determination of the elastic modulus can be derived from the stress-strain curve.

**Causes and Triggering Factors for Landslide at Fudale**

**Rainfall Analysis**

Rainfall in Fudale has increased since 2014, with the highest recorded in 2015. This led to increased ground surface fissures and decreased soil shear strength, resulting in landslides. The average annual rainfall is 1659 mm, with extremes of 2533 mm and 870 mm. A summary of the annual rainfall in Fudale is illustrated in Figure 4 below.

The monthly rainfall assessment in Fudale shows year-round precipitation, with low levels in January, February, and December, and the primary rainy seasons being April, May, August, September, October, and November. A summary of the monthly rainfall in Fudale is illustrated in Figure 5 below.


Figure 4: Annual rainfalls Analysis


Figure 5: Monthly Rainfall Analysis

**Slope Aspect**

The Digital Elevation Model (DEM) categorizes slopes into ten groups, with the southern slopes having the highest landslide occurrence at 36.2%. This is due to high weathering processes in the southern direction, reducing soil shear strength. The southern region of Ethiopia experiences the most intense solar radiation between 11:00 a.m. and 6:00 p.m., which increases weathering and contributes to landslide prevalence. The slope aspect of the research area is shown in figure 6.

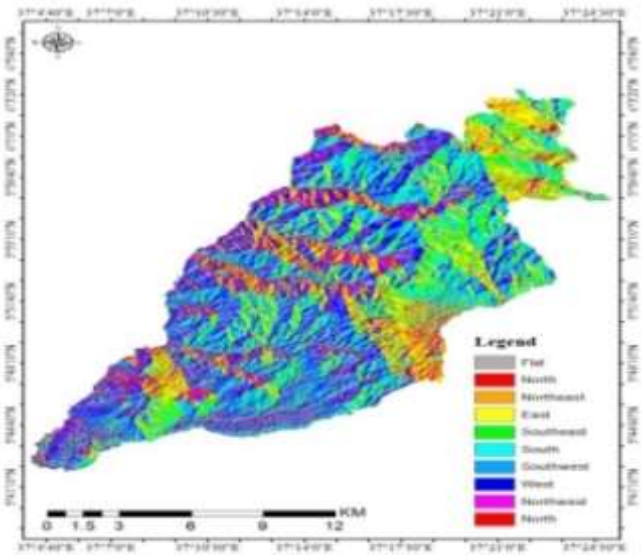


Figure 6: Slope aspect of the research area

**Curvature**

The research classified curvature into negative, flat, and positive values. Flat curvatures were more common for landslides, while convex and concave slopes experienced fewer. Concave slopes were more susceptible due to water concentration, while convex slopes had a lower probability of landslides due to uniform runoff distribution. The curvature of the research area is shown in figure 7.

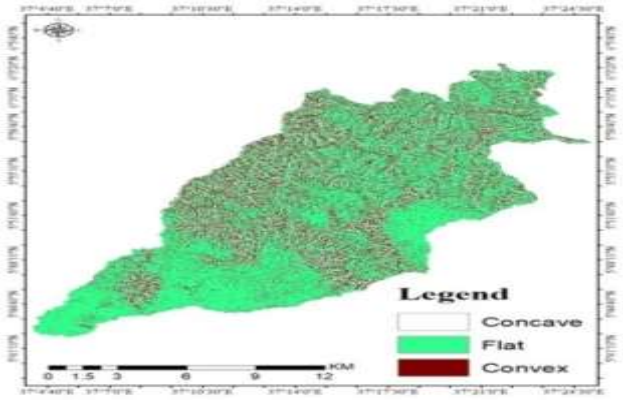

Figure 7: Curvature of the study area

**Slope Angle**

Shear stress increases the tangential component of the weight acting on the mass, while the perpendicular component declines faster. This results in the mass sliding on a slope. The DEM was used to derive slope data, which was categorized into five angles: (0-5)°, (5-12°), (12-20°), (20-25°), and (>25°). Landslides were most common in the slope range of 5-12° (62.6%), followed by less than 5° (25.3%). The slope angle of the research area is shown in figure 8.

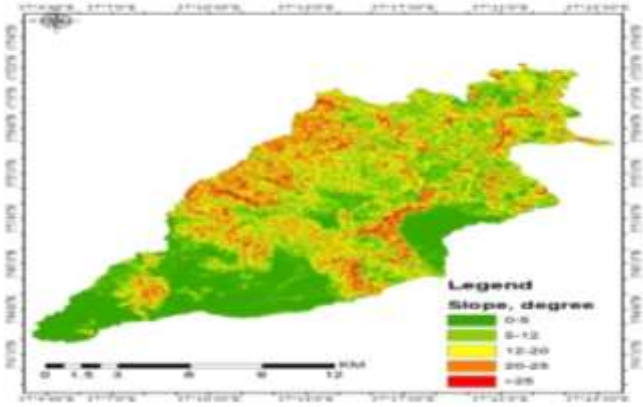

Figure 8: Slope angle map of the research area

**Influence of Soil Permeability**

Soil permeability is the ease with which water can flow through soil, influenced by factors like grain size and plasticity. In the Fudale, landslides, the soil was classified as clay and silty clay, with permeability ranging from 1.9*10^-6 to 4.7*10^-6 cm/sec. Differences in permeability between layers cause overburden movement, and the presence of springs or seepages indicates a permeable zone, decreasing soil permeability as depth increases.

**Slope Materials**

Soil properties vary based on factors like particle size, formation, shear strength, and water transmission. In Fudale, soils are classified as fine-grained, specifically highly plastic silt and highly plastic clay. These soils can lose strength when saturated, and their permeability coefficients vary between weathered and overburden clay materials. The presence of discontinuities in weathered rocks increases permeability, while water retention in fine-grained soils reduces permeability. These differences create pore pressures that trigger landslides, making soil characteristics a key factor in landslide incidence.

**Groundwater Condition and Elevation Difference**

Groundwater conditions are influenced by precipitation and elevation differences, leading to seepage, aquifer decreases, and runoff. Increased groundwater mass increases landslide risk, while fluctuations in pore water pressure negatively impact earth mass stability.

**Stream and Spring**

In the Fudale area, streams can cause landslides due to their role in eroding slopes during flood events, steepening the slope and removing support, despite large masses or underlying structures preventing the flow.

**Slope Stability Assessment with Plaxis 2D Software.**

**Geometrical Model of the Slope**

The study identified two layers of soil, one consisting of 6 meters of silty clay and the other 7 meters. The model was divided into two layers based on test pits' characteristics. The model covered 25 meters in length and reached 13 meters in height. The geometry and soil characteristics were based on geotechnical investigation. The Finite Element Method (FEM) was used for analysis, with initial stresses generated by gravity loading. The study used fine coarseness for mesh generation. The geometrical model of the slope of the research area is shown in figure 9.

**Material Modeling**

This research uses the elastic perfectly plastic Mohr-Coulomb model to investigate soil behavior, incorporating Young's modulus (E) and Poisson's ratio (v) for soil elasticity, internal friction angle (ϕ) and cohesion (c) for soil plasticity, and ψ for the angle of dilatancy. However, the model does not account for stiffness changes in response to stress and strain. The effective soil parameters are compiled in Table3.

Table 5: Soil parameters used in numerical modeling

| Sample Code | Description of soil | $\gamma$ sat (kN/m³) | $\gamma$ dry (kN/m³) | C (kN/m²) |
|---|---|---|---|---|
| Upper Layer | clayey and silt with high plasticity | 18.72 | 13.37 | 20.6 |
| Lower Layer | clayey and silt with high plasticity | 18.32 | 13.99 | 24.6 |

Table 6: Soil parameters used in numerical modeling

| Sample Code | Description of soil | Ø° | ψ° | E (Kpa) | ν |
|---|---|---|---|---|---|
| Upper Layer | clayey and silt with high plasticity | 12 | 0 | 4000 | 0.36 |
| Lower Layer | clayey and silt with high plasticity | 16.9 | 0 | 5000 | 0.34 |

**Boundary Condition of the Slope**

The slope's base was constrained in the X and Y axes, while the upper portion moved freely to accommodate soil deformation. The right side had a fixation along the X-axis. The boundary condition of the slope of the research area is shown in figure 10.

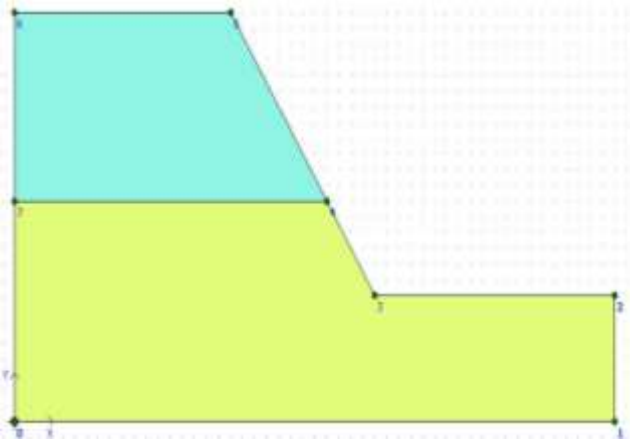

Figure 9: Geometrical model of the slope

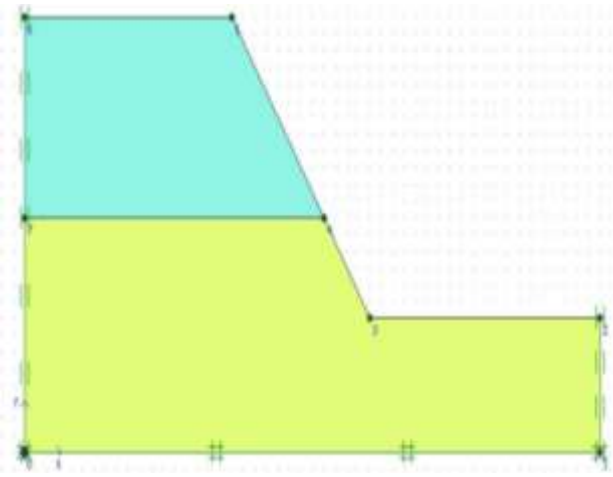

Figure 10: The Boundary Condition of the slope

**Mesh Generation**

The modeling process utilized fine mesh sizes with 305 soil elements, generated through an automatic unstructured mesh method, as shown in Figure 11.

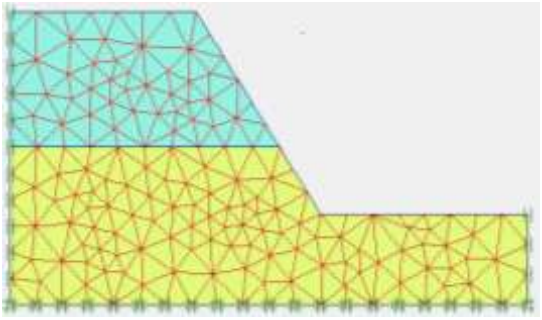

Figure 11: Meshing/ Discretization of the model

**Calculation with Plaxis-2D**

Plaxis offers computational options like plastic analysis, safety assessment, dynamic analysis, and flow-deformation analysis, based on loading and boundary conditions. Initial stress allocation is generated through gravity loading.

**Deformation Analysis and Result**

The deformation analysis was conducted using plastic calculation, focusing on an elastic-plastic deformation assessment with constant stiffness, and slope sections were evaluated under static loading conditions. The Deformation of the slope of the research area is shown in figure 12.

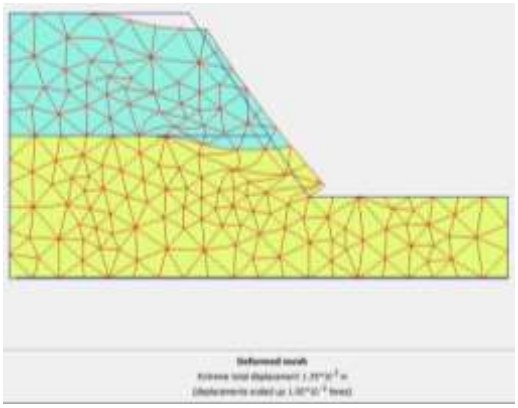

Figure 12: Deformation of slope

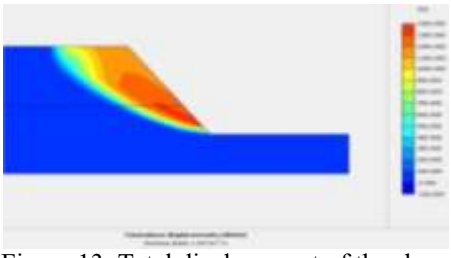

Figure 13: Total displacement of the slope

The upper part of the slope is known as the top side slope, which is the slope that is affected. The software analysis obtained a factor of safety result of 0.972 for this particular slope. Based on the criteria mentioned earlier, a factor of

safety of 0.972 indicates an unstable slope, which aligns with the current condition of the site. This slope is characterized by its steepness and is the most severely damaged slope within the study area.

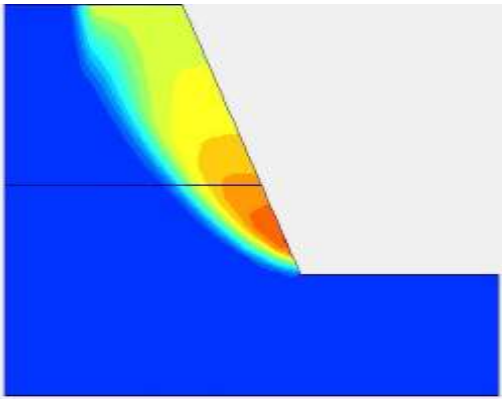

Figure 14: FOS output from software analysis

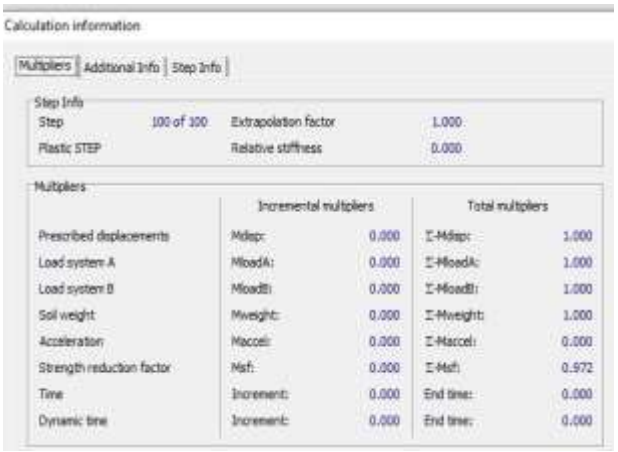


Figure 15: Calculation information of the software analysis

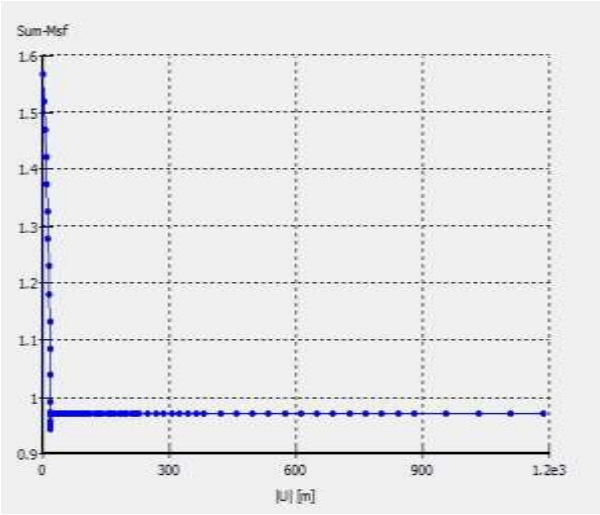


Figure 16: Safety Factor for Slope

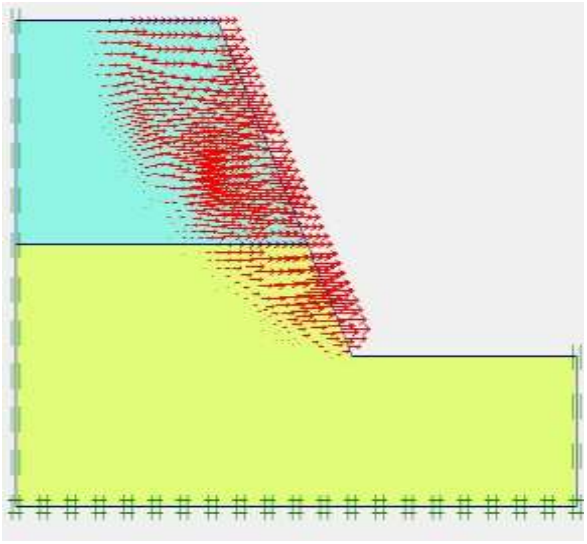

Figure 17: Direction of soil movement

The slopes' safety factor is unstable, with numerical values below 1, indicating increased water content during rainfall increases soil mass weight and reduces shear strength, potentially triggering landslides. Soil on a steep slope was prone to movement, causing significant damage to vegetation, animals, and human life. The software's results align with actual conditions at the site, as shown in Figure 16.

The analysis reveals peak deformation at the uppermost soil layer, specifically at the scarp, confirming field surveys and laboratory tests. The clayey silt layer is potentially unstable, with shallow failures and significant impact on slope stability during rainfall periods, despite not considering groundwater levels and GWT.

## IV. CONCLUSION

The study investigated soil characteristics and landslide stability in Fudale, focusing on fine-grained clay and silt soils. These soils are highly plastic and sensitive to moisture, exhibiting compressibility and swelling potential, leading to reduced shear strength when saturated, increasing the risk of landslides. Key factors contributing to landslide occurrences include intense rainfall, slope geometry, soil permeability, and groundwater conditions. The stability analysis indicated unstable conditions, causing land degradation, soil loss, and socio-economic issues, including infrastructure damage and disruptions to community activities. The soil's moisture content test results varied from 35.87% to 41.14%, and the specific gravity measurement indicated the soil's specific gravity range. The soil gradation test revealed 0.10%–0.80% gravel, 4.50%–7.38% sand, and 92.38%–95.06% fine soils. The dry unit weight ranged from 13.08 to 13.99 kN/m³, and the saturated unit weight ranged from 18.32 to 18.74 kN/m³. The triaxial test revealed a cohesion value of 28.02 to 57.60

kN/$m^2$, and the angle of internal friction values ranged from 9° to 16.94°. Over 92.38% of soil types were dominated by fine-grained soils, emphasizing the need for effective monitoring and management strategies to mitigate landslide risks in areas vulnerable to geological hazards.

**Acknowledgements**
The author expresses gratitude to God for providing courage, determination, and health throughout their life, as well as advisors Dr. Bisrat Gissila, Dr. Vasudeva Rao, and Democracy Dila for their support and guidance, parents for financial assistance, and friend Meron Abera for her constant encouragement and spiritual guidance in completing studies.

## REFERENCES

1. A. Serdarevic and F. Babic, "Landslide Causes and Corrective Measures – Case Study of the Sarajevo Canton," J. Civ. Eng. Res., vol. 9, no. 2, pp. 51–57, 2019,
2. L. M. Highland and P. Bobrowsky, "Introduction The Landslide Handbook-A Guide to Understanding Landslides," Landslide Handb. - A Guid. to Underst. Landslides, pp. 4–42, 2008.
3. P. Patra and R. Devi, "Assessment, prevention and mitigation of landslide hazard in the Lesser Himalaya of Himachal Pradesh," Environ. Socio-economic Stud., vol. 3, no. 3, pp. 1–11, 2015,
4. K. Woldearegay, "Review of the occurrences and influencing factors of landslides in the highlands of Ethiopia: With implications for infrastructural development," Momona Ethiop. J. Sci., vol. 5, no. 1, pp. 3–31, 2013,
5. D. M. Cruden, "The first classification of landslides?," Environ. Eng. Geosci., vol. 9, no. 3, pp. 197–200, 2003, doi: 10.2113/9.3.197.
6. G. Lollino et al., "Engineering geology for society and territory – Volume 2: Landslide processes," Eng. Geol. Soc. Territ. - Vol. 2 Landslide Process., vol. 2, pp. 1–2177, 2015,
7. A. J. T. Guerra, M. A. Fullen, M. do C. O. Jorge, J. F. R. Bezerra, and M. S. Shokr, "Slope Processes, Mass Movement and Soil Erosion: A Review," Pedosphere, vol. 27, no. 1, pp. 27–41, 2017,
8. D. P. Salunkhe, Assist. Prof. Guruprasd Chvan, Ms. Rupa N. Bartakke, and Ms. Pooja R Kothavale, "An Overview on Methods for Slope Stability Analysis," Int. J. Eng. Res., vol. V6, no. 03, pp. 528–535, 2017,
9. B. A. Yifru and F. M. Ayehu, "Prediction of Groundwater Level Fluctuation towards Rainfall Induced Landslide: Case of Blue Nile Gorge, Central Ethiopia," Open J. Mod. Hydrol., vol. 07, no. 04, pp. 274–297, 2017,
10. J. Liu, C. Yang, J. Gan, Y. Liu, L. Wei, and Q. Xie, "Stability Analysis of Road Embankment Slope Subjected to Rainfall Considering Runoff-Unsaturated Seepage and Unsaturated Fluid–Solid Coupling," Int. J. Civ. Eng., vol. 15, no. 6, pp. 865–876, 2017,
11. M. Geertsema, L. Highland, and L. Vaugeouis, "Environmental impact of landslides," Landslides - Disaster Risk Reduct., no. 1, pp. 589–607, 2009,
12. L. R. Walker and A. B. Shiels, "Chapter 3. Biological consequences for Landslide Ecology," Landslide Ecol., pp. 83–137, 2013.
13. A. W. Azeze, "Assessments of Geotechnical Condition of Landslide Sites and Slope Stability Analysis Using Limit Equilibrium Method around Gundwin Town Area, Northwestern Ethiopia," Res. Sq., 2020,